

PAPER

Epi-Intra neural probes with glassy carbon microelectrodes help elucidate neural coding and stimulus encoding in 3D volume of tissue

To cite this article: Nasim W Vahidi *et al* 2020 *J. Neural Eng.* 17 046005

View the [article online](#) for updates and enhancements.



The Department of Bioengineering at the University of Pittsburgh Swanson School of Engineering invites applications from accomplished individuals with a PhD or equivalent degree in bioengineering, biomedical engineering, or closely related disciplines for an open-rank, tenured/tenure-stream faculty position. We wish to recruit an individual with strong research accomplishments in Translational Bioengineering (i.e., leveraging basic science and engineering knowledge to develop innovative, translatable solutions impacting clinical practice and healthcare), with preference given to research focus on neuro-technologies, imaging, cardiovascular devices, and biomimetic and biorobotic design. It is expected that this individual will complement our current strengths in biomechanics, bioimaging, molecular, cellular, and systems engineering, medical product engineering, neural engineering, and tissue engineering and regenerative medicine. In addition, candidates must be committed to contributing to high quality education of a diverse student body at both the undergraduate and graduate levels.

[CLICK HERE FOR FURTHER DETAILS](#)

To ensure full consideration, applications must be received by June 30, 2019. However, applications will be reviewed as they are received. Early submission is highly encouraged.



PAPER

Epi-Intra neural probes with glassy carbon microelectrodes help elucidate neural coding and stimulus encoding in 3D volume of tissue

RECEIVED
13 May 2019REVISED
4 June 2020ACCEPTED FOR PUBLICATION
10 June 2020PUBLISHED
8 July 2020Nasim W Vahidi¹ , Srihita Rudraraju², Elisa Castagnola^{8,9} , Claudia Cea^{8,9}, Surabhi Nimbalkar^{8,9}, Rita Hanna^{8,9}, René Arvizu^{8,9}, Shadi A Dayeh^{1,3,4}, Timothy Q Gentner^{5,6,7} and Sam Kassegne^{8,9,10} ¹ Department of Electrical and Computer Engineering, University of California San Diego, La Jolla, CA 92093, United States of America² Department of Bioengineering, University of California San Diego, La Jolla, CA 92093, United States of America³ Materials Science and Engineering Program, University of California San Diego, La Jolla, CA 92093, United States of America⁴ Department of Nanoengineering, University of California San Diego, La Jolla, CA 92093, United States of America⁵ Neurosciences Graduate Program, University of California San Diego, CA 92093, United States of America⁶ Department of Psychology, University of California San Diego, La Jolla, CA 92093, United States of America⁷ Neurobiology Section, Division of Biological Sciences University of California San Diego, La Jolla, CA 92093, United States of America⁸ NanoFab.SDSU Lab., Department of Mechanical Engineering, College of Engineering, San Diego State University, 5500 Campanile Drive, San Diego, CA 92182-1323, United States of America⁹ Center for Neurotechnology (CNT), Box 37, Bill & Melinda Gates Center for Computer Science & Engineering, 3800 E Stevens Way NE, Seattle, WA 98195, United States of America¹⁰ Author to whom any correspondence should be addressed.E-mail: kassegne@sdsu.edu**Keywords:** neural probes, microelectrodes, multi-functional probes, origami structures, MEMS

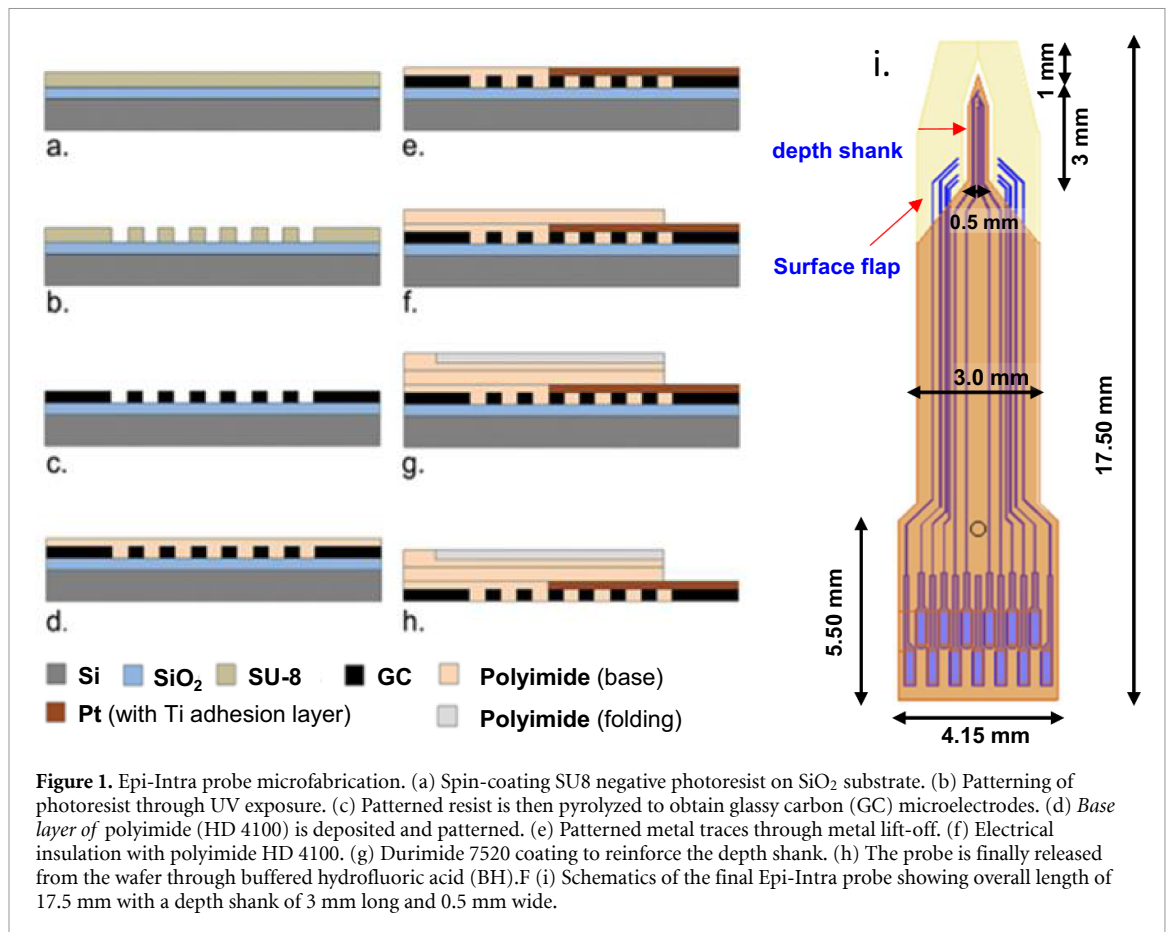
Abstract

Objective. In this study, we demonstrate practical applications of a novel 3-dimensional neural probe for simultaneous electrophysiological recordings from the surface of the brain as well as deep intra-cortical tissue. We used this 3D probe to investigate signal propagation mechanisms between neuronal cells and their responses to stimuli in a 3D fashion. **Approach.** This novel probe leverage 2D thin-film microfabrication technique to combine an **epi**-cortical (surface) and an **intra**-cortical (depth) microelectrode arrays (**Epi-Intra**), that unfold into an origami 3D-like probe during brain implantation. The flexible epi-cortical component conforms to the brain surface while the intra-cortical array is reinforced with stiffer durimide polymer layer for ease of tissue penetration. The microelectrodes are made of glassy carbon material that is biocompatible and has low electrochemical impedance that is important for high fidelity neuronal recordings. These recordings were performed on the auditory region of anesthetized European starling songbirds during playback of conspecific songs as auditory stimuli. **Main results.** The Epi-Intra probe recorded broadband activity including local field potentials (LFPs) signals as well as single-unit activity and multi-unit activity from both surface and deep brain. The majority of recorded cellular activities were stimulus-locked and exhibited low noise. Notably, while LFPs recorded on surface and depth electrodes did not exhibit strong correlation, composite receptive fields (CRFs)—extracted from individual neuron cells through a non-linear model and that are cell-dependent—were correlated. **Significance.** These findings demonstrate that CRFs extracted from Epi-Intra recordings are excellent candidates for neural coding and for understanding the relationship between sensory neuronal responses and their stimuli (stimulus encoding). Beyond CRFs, this novel neural probe may enable new spatiotemporal 3D volumetric mapping to address, with cellular resolution, how the brain coordinates function.

1. Introduction

The last decade witnessed an explosion of interest in microelectrode arrays that can record hundreds

to thousands of neurons across cortical layers [1, 2]. Surface recordings have followed these footsteps and recently enabled recordings from thousands of contacts [3]. In other studies, surface recordings



advanced to resolve single unit activity from the surface of the brain in animals and humans [4–6]. To investigate the inter-relationship between surface and depth recordings, separate surface and depth electrodes are typically used [7, 8]. Single composite surface/depth (epicortical/intracortical) array that can uncover the spatiotemporal and neurophysiological correlations between surface and depth recordings are rare. Recently, we introduced of a new pattern transfer technology that allowed glassy carbon (GC) structures to be supported on polymeric substrates enabling the microfabrication of GC microelectrodes of increasingly complex shapes [9, 10]. One such design that addresses the need for a composite surface and depth electrode involves 3D origami-style probes that are fabricated on a flexible polymer substrate using thin-film microfabrication techniques that are capable of reshaping into 3D structures. Based on this approach, we demonstrated a neural probe made of a microelectrode array platform that integrates both surface (epicortical) and penetrating (intracortical) GC electrodes onto a single flexible thin-film device [11]. Additionally, we demonstrated that these flexible GC microelectrodes are capable of sustaining in excess of 3.5 billion cycles of bi-phasic pulses at charge density of 0.25 mC cm^{-2} , confirming remarkable longevity of these microelectrodes under stimulation stresses [12].

Here, we leverage our 3D origami-style probes to incorporate a lithographically-defined stiffer polymer that forms the penetrating shank component of these probes to encompass an **epi**-cortical surface microelectrode array and an **intra**-cortical depth microelectrode array (hence, the name Epi-Intra) for volumetric brain recording. The proof of principle Epi-Intra electrode consists of four GC epi-recording contacts and eight GC intra-recording contacts on a flexible polymer substrate. To enable volumetric brain recording, the epi-recording microelectrodes are positioned on both left and right side of intracortical electrode (figures 1 and 3). Using this new Epi-Intra probe, therefore, we explore its capabilities as potential tool for neural coding (stimulus processing by neurons) and stimulus encoding or stimulus reconstruction (mapping stimuli to recorded neural responses) from deep brain to cortical surface and elucidating brain responses in a 3D fashion. With stimulus encoding thus obtained, we intend to reconstruct stimuli from neural responses [13–15].

The core Carbon-MEMS microfabrication technology that is used for these GC probes is described in detail elsewhere [9–11]. This current work extends this technology to incorporate shanks with graded mechanical stiffness. The new extended microfabrication method is discussed in detail in the Methods section. To demonstrate its utility in shedding new

light on fundamental neuroscience questions, the 3D Epi-Intra probe is used to investigate the relationship between stimuli and brain responses across surface and depth. We particularly focus on the determining the possible correlation between local field potentials (LFPs) from epicortical microelectrodes and action potentials recorded by intracortical microelectrodes located in the shank. Here, we examine the suitability of composite receptive fields (CRFs) approach to benchmark evoked cellular responses at the surface versus the depth of brain tissue and determine their correlation.

2. Methods

2.1. Epi-Intra neural probe microfabrication

Recently, we introduced a novel technology for transferring GC probes from a carrier silicon wafer to a polymeric flexible substrate such as polyimide [9]. This new transfer technique addressed a major barrier in Carbon-MEMS technology whose widespread use has been hampered by the high-temperature pyrolysis process ($\geq 900^\circ\text{C}$), which limits selection of substrates. In this new approach, patterning and pyrolysis of polymer precursor on the silicon substrate is carried out first, followed by coating with a polymer layer that forms hydrogen bonds with glassy carbon [16]. The ensuing glassy carbon structure is then released; hence, transferring it to a flexible substrate. This enables the fabrication of a unique set of glassy carbon microstructures critical in applications that demand substrates that conform to the shape of the interrogated surface.

Subsequently, for applications requiring 3D data recording, we then integrated the GC sensing microelectrodes into 3D origami-style platform. Here, we discuss the details of the modified microfabrication method that now allows extra processes that are added to offer a stiffness-graded neural probe with a stiff shank for penetrating brain tissue and a soft and compliant flap that sits on the cortex. The microfabrication process starts by spin-coating $10\ \mu\text{m}$ thick SU8 negative photoresist (Microchem, MA) on SiO_2 substrate at 1000 rpm for 55 s (figure 1(a)). The coated substrate was soft-baked at 65°C for 10 min and then at 95°C for 20 min, followed by UV exposure at an intensity of $\sim 400\ \text{mJ cm}^{-2}$. Further, post-exposure bake was run at 65°C for 1 min and 95°C for 1 min. This was followed by development of SU8 layer to define the SU8 microelectrode-like patterns shown in figure 1(b). Pyrolysis was done at 1000°C in an inert N_2 environment following protocols described elsewhere [9–12] resulting in GC microelectrodes with a thickness of $2\ \mu\text{m}$ (figure 1(c)). Then $10\ \mu\text{m}$ layer of photo-patternable polyimide HD 4100 (HD Microsystems, DE, USA) was spin-coated on top of GC microelectrodes at 2500 rpm for 45 s, soft baked at 90°C for 6 min, then cooled to

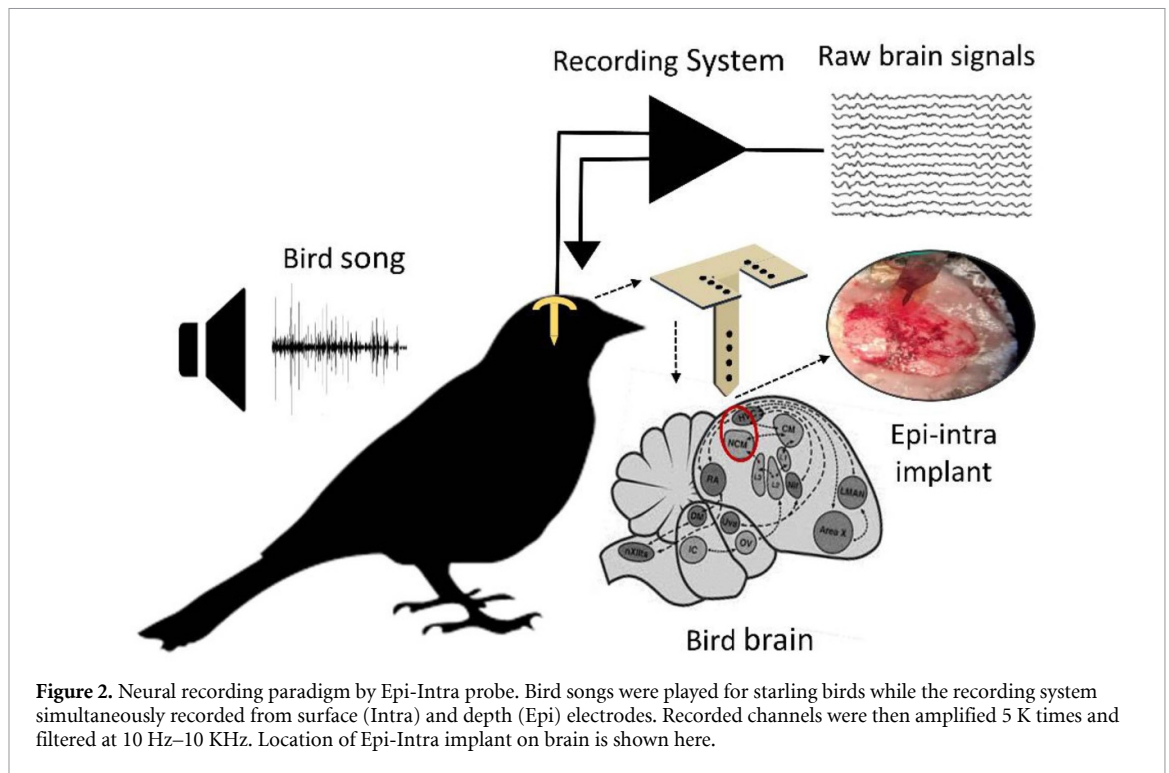
room temperature, and patterned through UV exposure at $\sim 400\ \text{mJ cm}^{-2}$. This was followed by partially curing at 300°C for 60 min in N_2 environment resulting in a structure that is schematically illustrated in figure 1(d). Following this, Pt metal traces were patterned using lift-off process with a sacrificial layer of NR9-1000PY photoresist (Futurrex, Inc. USA). Ti adhesion layer of 20 nm and 200 nm Pt layer were deposited through sputtering (figure 1(e)). For electrical insulation, an additional $8\ \mu\text{m}$ of polyimide HD 4100 (300 rpms) was spun-cast, patterned ($400\ \text{mJ cm}^{-2}$), and cured (350°C for 90 min) in N_2 environment (figure 1(f)). Finally, $30\ \mu\text{m}$ thicker layer of polyimide (Durimide 7520, Fuji Film) was spin-coated (800 rpm, 45 s) and then patterned ($400\ \text{mJ cm}^{-2}$) on top of the insulation layer to reinforce the penetrating portion of the probe (figure 1(g)). Finally, the $\sim 50\ \mu\text{m}$ thick probe was released from the wafer through selective etching of silicon dioxide layer with buffered hydrofluoric (BHF) acid (figure 1(h)).

2.2. Mechanical characterizations

Finite element modeling (FEM) was carried out to (a) determine the compliance of the folding polyimide flap that contains the surface microelectrodes as the shank is inserted in the brain tissue and (b) determine the stresses induced during deployment of the whole probe and hence its robustness in handling loads. COMSOL Multiphysics FEM program (COMSOL AB, Sweden) was used for building three-dimensional finite element model of the probe ($50\ \mu\text{m}$ thick) consisting of 30 215 tetrahedral elements subjected to a total 10 millinewton applied as a surface load on the flap. The load level is considered appropriate for *in vivo* insertion procedure. The bottom of the probe was considered fixed. Due to the large displacements involved, a geometrically non-linear analysis with the surface load remaining tangential to the surface of the flap was considered. Further, to measure the load carrying capacity of the probe and determine its composite modulus, Instron's 1500HDX Universal Testing Machine (Instron, USA) was used where tensile load was applied on the shank component until failure, and the resulting extension measured. Threadrolled C-clamps that provide greater precision for easy adjustment of position were used to grip the probe [12]. The frame of C-clamps was then held between the jaws of upper and lower clamps of the Instron machine. The cross-head extension rate was set at $0.5\ \text{mm min}^{-1}$. The specimen was then loaded to failure at this rate and the load-deflection curve plotted. Young's Modulus was determined by taking the mean slope of ten points in the elastic region of the stress-strain curve.

2.3. Electrical characterizations

Electrochemical impedance spectroscopy (EIS) was used to determine the electrochemical properties of

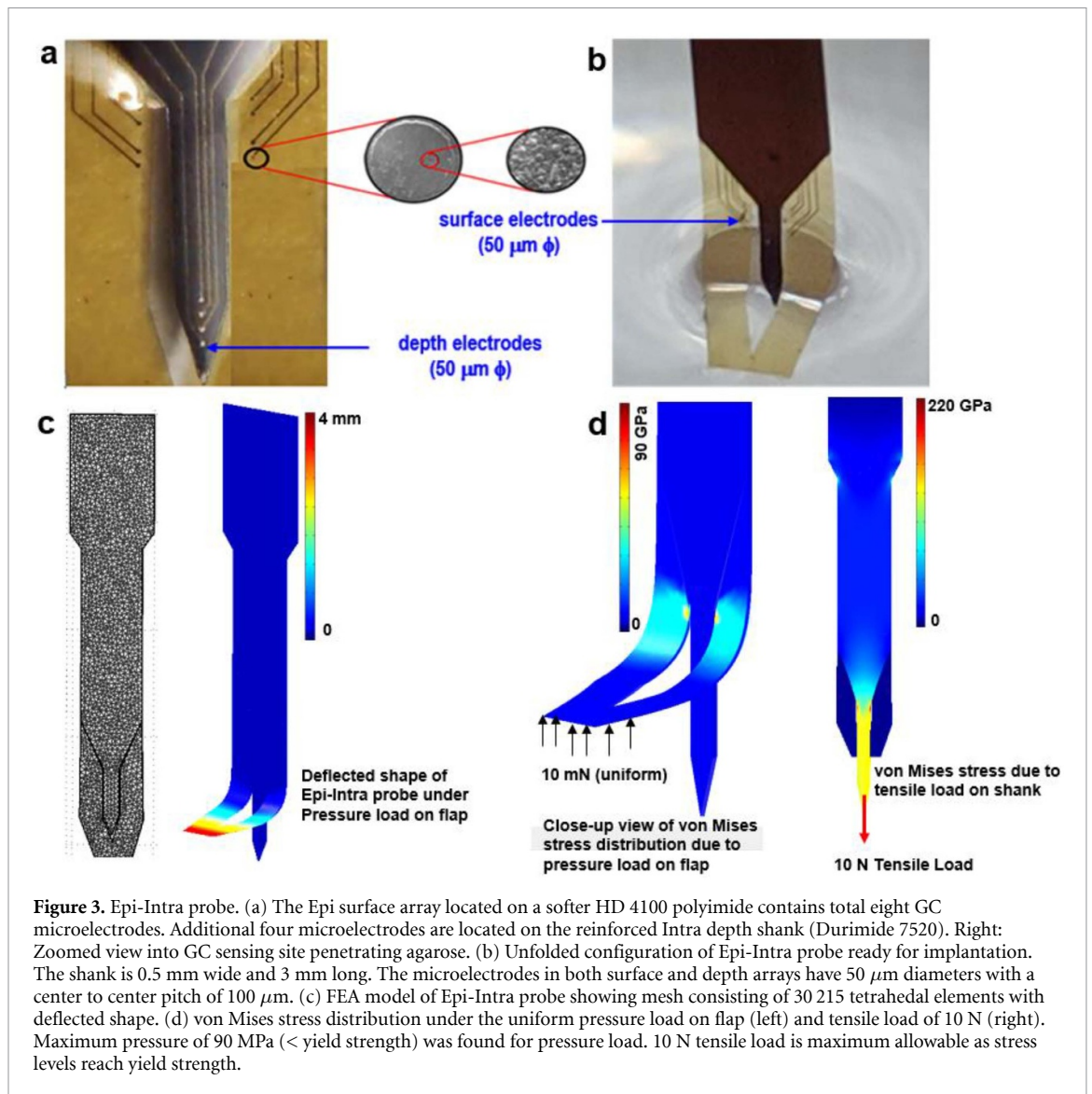


the microelectrodes (bode plots and impedance) in the frequency range of 0.1 Hz–100 kHz using a potentiostat (Reference 600+, Gamry Instruments, USA) connected to a three-electrode electrochemical cell with a platinum wire as a counter electrode and a saturated Ag/AgCl reference electrode. Phosphate-Buffered Saline solution (PBS; 0.01 M, pH 7.4; Sigma Aldrich, USA) was used as a buffer solution. For EIS measurements, 10 mV RMS amplitude sine wave was superimposed on 0 V potential with frequency sweep from 0.1 to 10^5 Hz.

2.4. Surgical procedure and electrophysiology

Experiments were performed on three adult European starling songbirds under a protocol approved by the Institutional Animal Care and Use Committee of the University of California, San Diego. Isoflurane and urethane ($7\text{--}8\text{ ml kg}^{-1}$) were used to obtain active auditory response while subjects were under anesthesia [17]. Following this, subjects were placed in a stereotaxic apparatus inside a sound attenuation chamber. A small craniotomy was made on Caudomedial Nidopallium (NCM) auditory area and the dura was removed. Subsequently, Epi-Intra electrode combinations were advanced into the brain at the coordinate of 500–1000 μm caudal and 500–1000 μm lateral on right side of Y-sinusous. Intra depth electrode was lowered 3000 μm deep until the epi surface array touched and conformed onto the cortex. Then, five starling bird songs were played 20 times randomly for the subjects. The songs were played randomly to prevent gradual stimulus

adaptation by subjects [18]. These bird song stimuli were recorded from starling males at 44.1 thousand samples s^{-1} and played back for the subjects at 60 dB. Figure 2 shows this recording paradigm. While bird song stimuli were played for the anesthetized birds in a sound chamber, the neural data was simultaneously recorded from eleven channels of Epi-Intra electrodes: Seven channels recorded signals from brain surface and four channels recorded signals from depth brain. The data was amplified by an amplifier system (A-M model 3600) with a gain of 5 K, sampling rate of 20 KHz, and then low and high pass filtered respectively at 10 Hz and 10 KHz. The recorded data was then converted to Matlab files. As a control for Epi-Intra recordings, they were compared with commercial 32-channel depth electrode (NeuroNexus A1x32-Edge-10 mm-20-177) recordings from the same NCM auditory region. The recording sites on these commercial electrodes have 20 μm spacing with a 177 μm^2 surface area and are made of iridium. The results show that the quality of the intra-cortical recordings is comparable with the commercial electrode recordings. The recorded data then was divided onto two data sets. By filtering data less than 300 Hz, we collected local field potential (LFP) signals and by filtering data above 300 Hz, we isolated high frequency data that was used for cell sorting. To extract cells from high frequency data, MountainSort program was utilized. This program is a clustering algorithm which works with high-dimensional data to sort neuronal cells [19]. Following this, the clusters containing noise were disregarded and the sorted neural cells were grouped to single cells and multi-units. The signal



processing analysis in this study was performed in MATLAB software (Mathworks, USA) and python.

3. Results

Figures 3(a) and (b) show the Epi-Intra probe micro-fabricated for this study. The overall length of the probe is 17.5 mm with a depth shank of 3 mm long and 0.5 mm wide. The width of the probe is on the higher side and could be reduced to as low as 0.25 mm. The Epi-Intra probe which has the ability to unfold to a combination of a surface ECoG array and a penetrating depth shank has a total of twelve GC microelectrodes of 50 μm diameter and 100 μm center to center pitch. The eight surface GC microelectrodes are separated into two parts around the depth shank as shown in figure 3(a). These two surface arrays in both sides of depth shank increase the chance of recording from a broader area of the cortex. Their combination with the depth shank will also cover a 3D volume of brain tissue, which is the objective of this study. The intra depth shank, on the other

hand, contains four GC sensing microelectrodes on a reinforced polyimide shank. After implanting the Epi-Intra probes, *in vivo* characterization was performed. Optical images of the probe demonstrated an intact uniform distribution of the glassy carbon microelectrodes before and after implantation (figure 3(a) right). Further, the GC penetrating microelectrodes did not exhibit a significant change in impedance before or after implantation.

3.1. Mechanical characterizations

Figure 3(c) shows the FEM results of displacement of the polyimide flap under the uniform pressure load applied at the bottom. The model demonstrates that for complete opening of the polyimide flap component of the Epi-Intra probe (i.e. out-of-plane displacement of 3 mm), a total load of 10 millinewton applied as a pressure load is needed. This corresponds to a compliance of ~ 0.33 mm millinewton $^{-1}$, which is within the range of what is typical for flexible neural probes. Further, the *von Mises* stress distribution shown in figure 3(d) indicates that the maximum

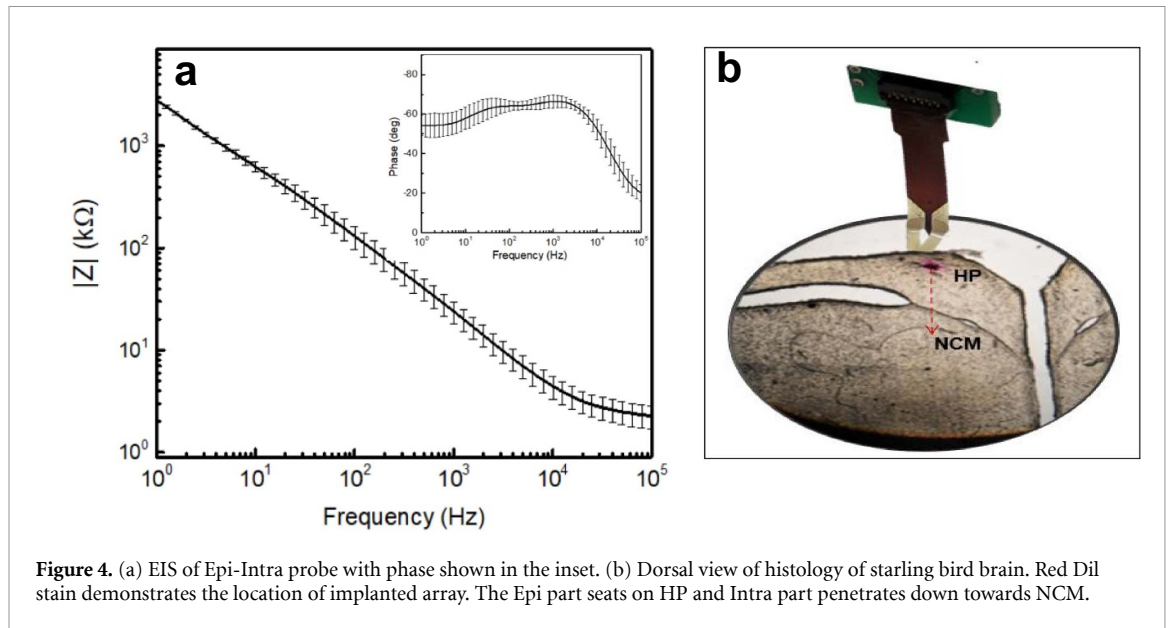


Figure 4. (a) EIS of Epi-Intra probe with phase shown in the inset. (b) Dorsal view of histology of starling bird brain. Red Dil stain demonstrates the location of implanted array. The Epi part seats on HP and Intra part penetrates down towards NCM.

stress (~ 90 MPa) occurs, as expected, at a corner where the compliant polyimide flap meets the stiffer penetrating shank made of durimide. This is much less than the tensile yield strength of 200 MPa [20]. Further, FEA model with tensile load matched closely the ultimate load of 10 N that is found by our mechanical tensile load test which had similar load deflection behavior as our previously reported result with durimide 7520 polymer substrate [12]. The Young's Modulus of the composite structure consisting of two layers of polyimide (HD 4100), metal traces, and a final layer of stiffer durimide 7520 was found to be ~ 2.35 GPa which is expected as the modulus of the thicker durimide 7520 by itself is 2.5 GPa [21]. Histological analysis was also carried out to investigate the location of inserted shank as well as to explore the degree of tissue damage during the acute *in vivo* experiments. The brain tissues were cut horizontally/parallel to the rostral-caudal axis of the brain. Figure 4(b) demonstrates that tissue injury is minimal and within a normal range, similar to the effect produced by the control commercial probes used. We also carried out a buckling analysis to determine if such instability could occur under compressive insertion loads during surgical implanting of the probe. The Euler buckling load formula for rods fixed on one end and subjected to a compressive load on the free end was considered (i.e. $K = 0.7$) as shown in equation (1).

$$P_{cr} = (\pi^2 EI) / (L)^2 \quad (1)$$

Where P_{cr} is Euler's critical load, E is Young's modulus (2.5 GPa), I is moment of inertia, and L is length of the rod (4 mm). The minimum buckling load corresponds to the minimum (weak-axis) moment of inertia with width = 0.5 mm and depth = $50 \mu\text{m}$ giving $I = 4.185 \times 10^{-8} \text{ m}^4$ (i.e. $bd^3/12 = (0.0005 \text{ m}) \cdot (0.00005 \text{ m})^3/12$). For these

conditions, $P_{cr} = 16.4 \text{ mN}$, which is larger than the total insertion load of 10 mN considered here.

3.2. Electrochemical characterizations

Electrochemical characterization for the penetrating results is shown in figure 4(a). The impedance values at 10 Hz, 100 Hz and 1 kHz are $(650.5 \pm 25.6) \text{ k}\Omega$, $(105.5 \pm 15.9) \text{ k}\Omega$ and $(22 \pm 2.2) \text{ k}\Omega$, respectively (mean and standard deviation, $n = 10$). These indicate an excellent range for neural recording applications for microelectrodes with $50 \mu\text{m}$ diameter [22].

3.3. Statistical analysis of electrophysiological recordings

In addition to the previously reported compelling properties of GC microelectrodes which were shown to offer high-resolution chemical and neurotransmitter detection, GC microelectrodes on Epi-Intra probe used in this study demonstrated exceptional potential in electrical recording from the auditory area of starling bird brains.

Figure 5 displays an example of high pass signals of eleven channels recorded simultaneously from the surface of the brain by the Epi array in red and from deep brain by the Intra shank in blue. The twelfth channel on the surface was used as a reference electrode. On top of the figure, a spectrogram of a 15 s bird song is displayed which demonstrates modulation of bird song power over time, across twenty frequencies. The color bar next to the song spectrogram indicates the song power intensity. By analyzing the high pass signals, we were able to detect multiple clusters of single cell as well as multi-unit recordings. Figures 6(b)–(f) demonstrates example waveforms of a few single cells that are recorded by GC microelectrode from surface (figure 6(b)) and deep brain (figure 6(f)). To differentiate between single cells and

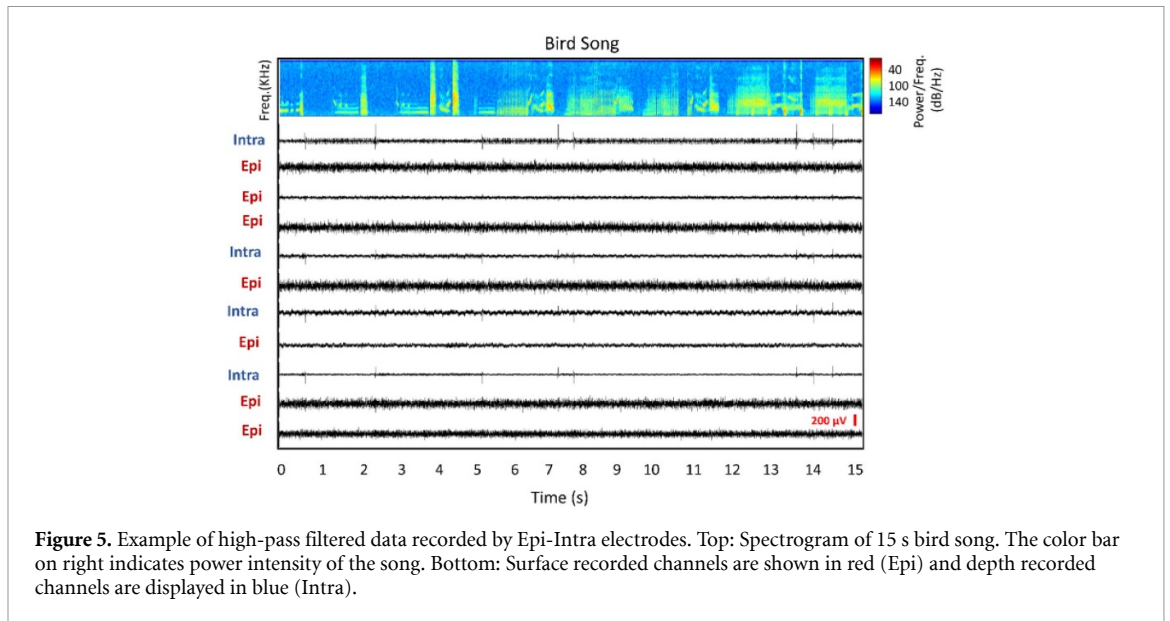


Figure 5. Example of high-pass filtered data recorded by Epi-Intra electrodes. Top: Spectrogram of 15 s bird song. The color bar on right indicates power intensity of the song. Bottom: Surface recorded channels are shown in red (Epi) and depth recorded channels are displayed in blue (Intra).

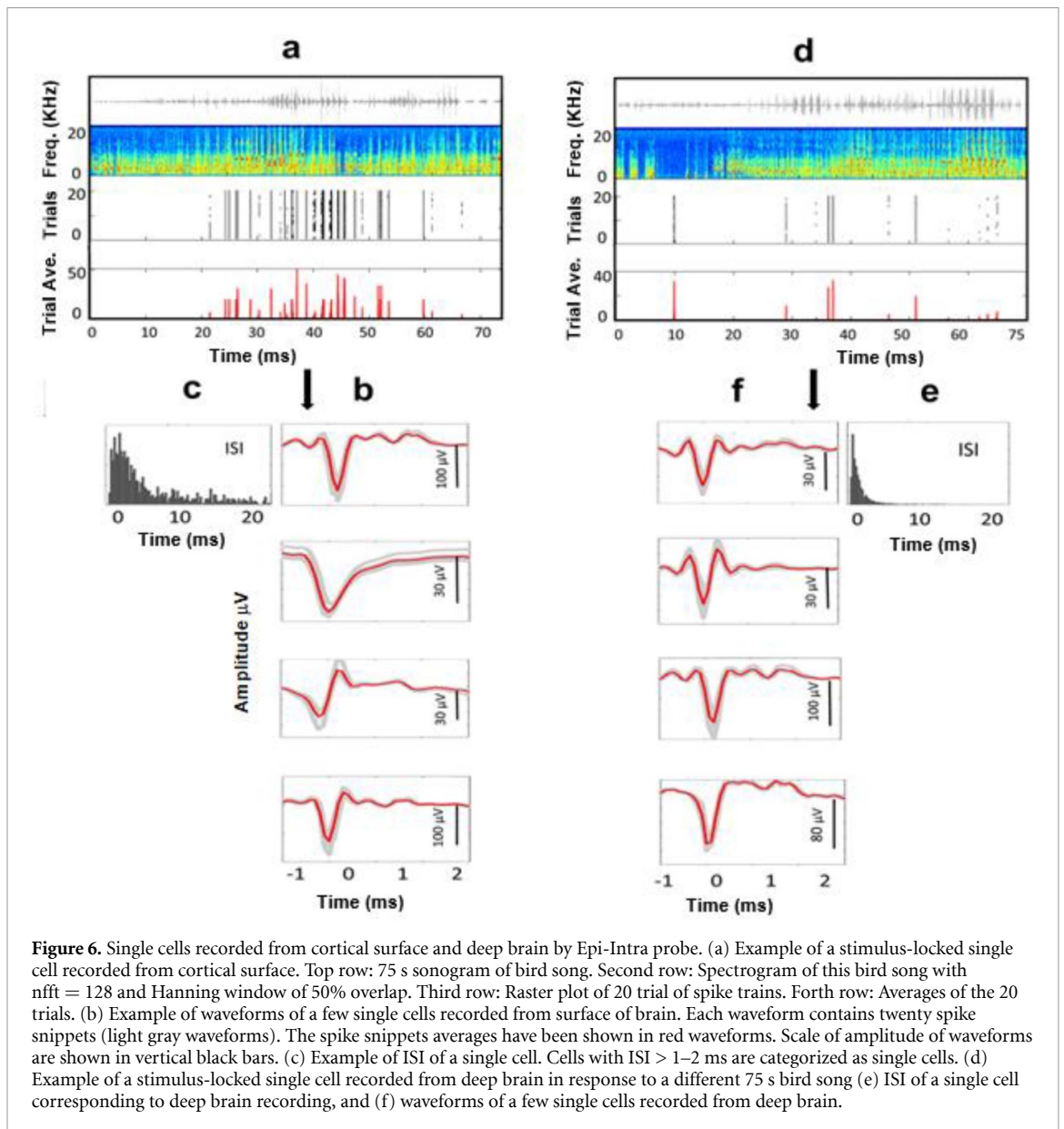
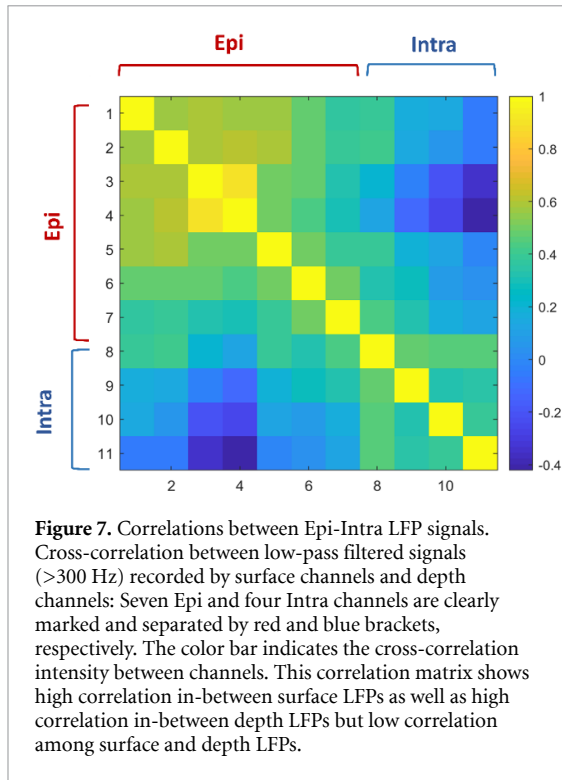


Figure 6. Single cells recorded from cortical surface and deep brain by Epi-Intra probe. (a) Example of a stimulus-locked single cell recorded from cortical surface. Top row: 75 s sonogram of bird song. Second row: Spectrogram of this bird song with $nfft = 128$ and Hanning window of 50% overlap. Third row: Raster plot of 20 trial of spike trains. Forth row: Averages of the 20 trials. (b) Example of waveforms of a few single cells recorded from surface of brain. Each waveform contains twenty spike snippets (light gray waveforms). The spike snippets averages have been shown in red waveforms. Scale of amplitude of waveforms are shown in vertical black bars. (c) Example of ISI of a single cell. Cells with $ISI > 1-2$ ms are categorized as single cells. (d) Example of a stimulus-locked single cell recorded from deep brain in response to a different 75 s bird song (e) ISI of a single cell corresponding to deep brain recording, and (f) waveforms of a few single cells recorded from deep brain.



multi-units, cells inter spike intervals (ISI) were calculated. Cells with ISI more than 1–2 ms were categorized as single cells [23]. Figures 6(c)–(e) display example of ISI related to two single cell waveforms recorded from the surface and depth of the brain.

In figure 6(a), the right and left raster plots that correspond to the above two single cells are shown. The top rows show 70 s and 75 s sonogram, amplitude modulation, of two bird song stimuli. The second row shows a spectrogram of these bird songs with $nfft = 128$ and Hanning window of 128 with 50% overlap. The third row displays 20 trials of spike trains, while the fourth row shows the averages of these 20 trials. These plots (figures 6(a)–(d)) provide evidence that significantly stimulus-locked cells with minimum noise were recorded from auditory neurons from deep brain and cortical surface [24].

To examine the Epi-Intra probe's 3D configuration as a possible tool for neural coding and stimulus encoding over a 3D region of brain tissue, we first attempted to investigate cross-correlation of LFP signals recorded by surface and depth channels. Figure 7 demonstrates the correlation matrix between seven surface channels and four depth channels. Seven Epi and four Intra channels are indicated by red and blue brackets, respectively. This correlation matrix demonstrates that, although there are high correlation in-between surface Epi channels and in-between Intra depth channels, the correlation is relatively low among surface and depth channels. In fact, cross-correlation across channels decrease when distance between channels are more than 1500 μm . This

finding agrees well with results reported by other investigations such as [25, 26].

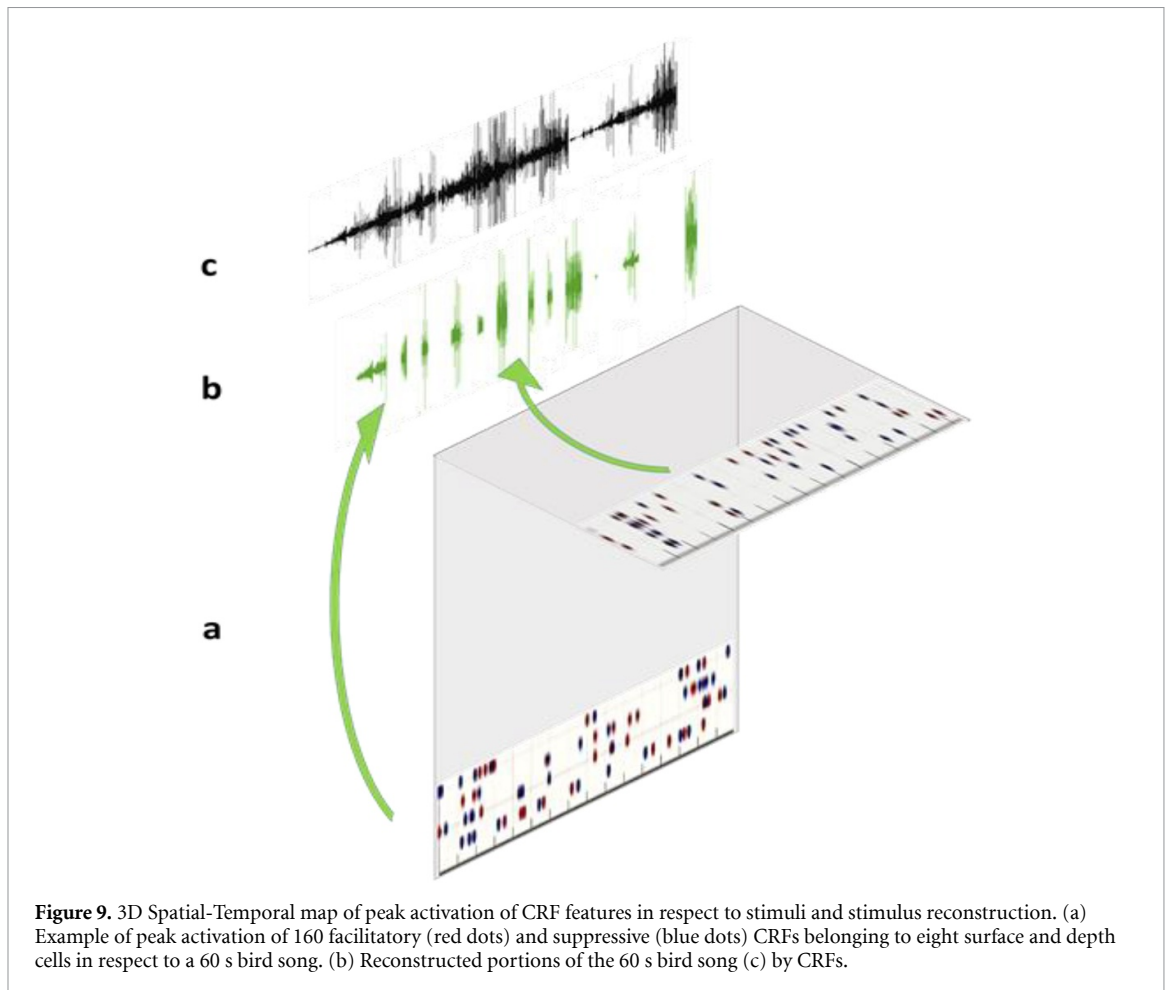
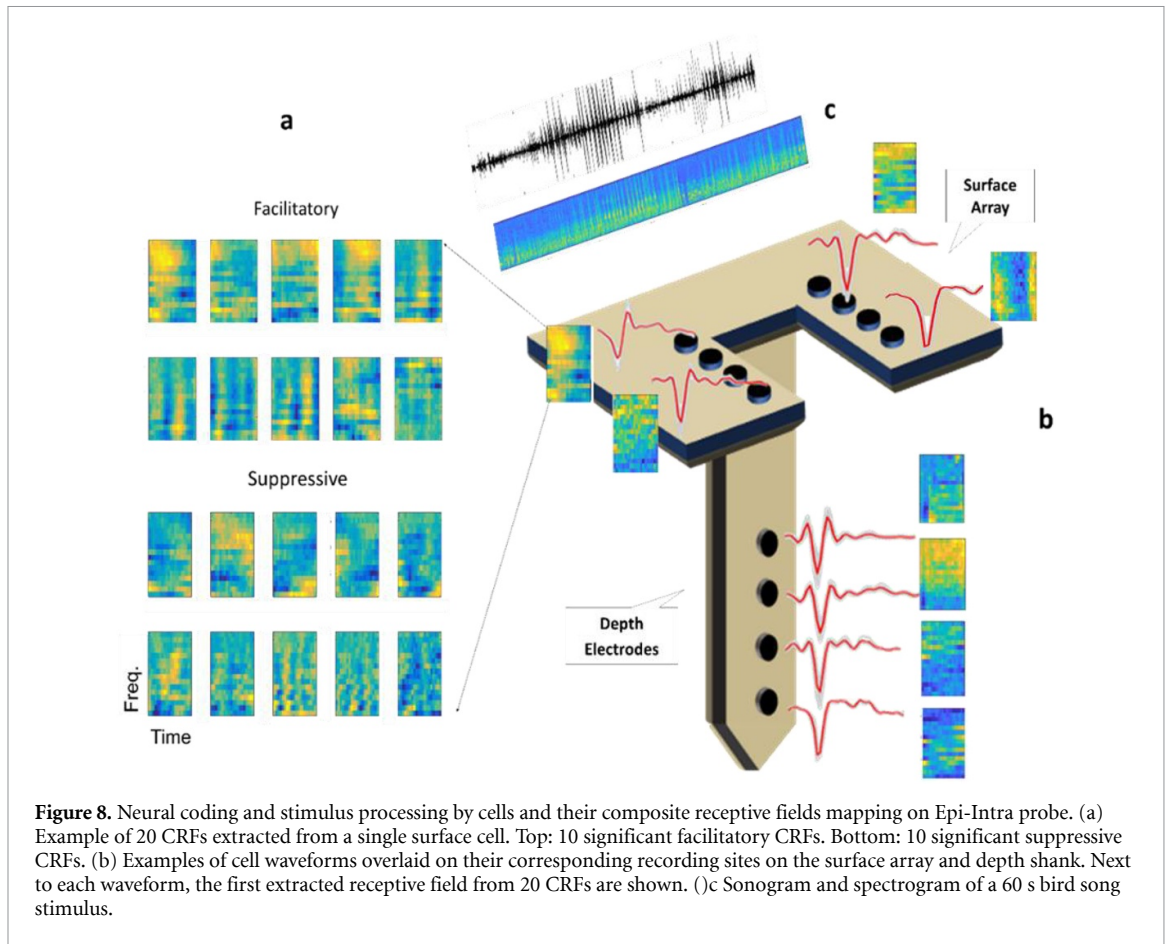
Faced with this challenge of decreasing cross-correlation of LFPs with distance, we, therefore, then proposed the investigation of an alternate approach involving composite receptive fields (CRFs) of neuron cells [27]. In a recent study, we already have shown that CRFs are independent of the neurons' location and their topology [28]. CRFs, therefore, appear, at least theoretically, to offer a potentially useful tool for investigating the usefulness of the Epi-Intra probe as a tool for neural coding over a larger brain area.

As starters, to extract high quality composite receptive fields from neuron cell responses, the cell responses should be stimulus-locked with low noise [27, 28]. Since the recorded cells by Epi-Intra probe exhibit such properties, as shown earlier, we were then able to extract CRFs from them quite easily. To generate CRFs from the recorded cells, maximum noise entropy model (MNE) was adopted [27, 29]. This model generates receptive fields from mutual information between neuron cells response and their stimuli. Stimuli spectrogram power density and the neuron cells response average over 20 trials are two inputs of the MNE model. To build stimuli spectrograms power density, first bird songs were down-sampled to 24 KHz, the DC part of signal was removed, and the adjacent 64 frequencies are averaged pairwise twice to receive 16 frequency bands with band ranges of 750 Hz–12 KHz (Nyquist frequency). Time bins were down-sampled to similar frequency to extract 20 bins. Following, the power spectral density (PSD) of the spectrogram was extracted (figures 6(a)–(d) second row). To construct the neuron cell response, an average of 20 trial responses for each cell were calculated (figures 6(a)–(d) fourth row). These two data sets were then divided to sets of test and train and have been pushed to the MNE logistic model (equation (2)).

$$P(\text{Response}|\text{Stimuli}) = \left(1 + e^{f(s)}\right)^{-1} \quad (2)$$

In this equation, the polynomial equation $f(s) = (a + hs + s^T J s)$ was minimized and parameters a , h , and J estimated, where a , h , and J correspond respectively to the constant, linear part, and quadratic part of receptive field features. The quadratic J contains eigenvalues and eigenvectors. CRFs shown in figure 8(a) were extracted from a single surface cell and they were built from twenty eigenvectors of J -matrix that are significant, out of which ten are facilitatory and the other ten represent suppressive receptive fields. Significant eigenvectors have the highest (negative) or lowest probability (positive) of occurring on the logistic MNE function.

Furthermore, negative and positive eigenvectors correspond to facilitatory and suppressive CRFs



successively (figure 8(a) top and bottom) [27]. This analysis was performed on the stimulus-locked cells and subsequently generated twenty CRFs per cell. To validate this result, the commercial control electrodes recorded CRFs and the Epi-Intra probe CRFs were compared and the results were found to be quite comparable. Figure 8(b) displays Epi-Intra combination electrodes with the example of single cell waveforms from their corresponding recording sites on the surface array and depth electrode. Next to each waveform, the first extracted receptive field from 20 CRFs are shown. To investigate the spatial-temporal map of CRFs in a 3D volume of tissue, we first extracted 20 facilitatory and suppressive CRFs from these eight cells recorded from surface and deep brain, which yielded 160 CRFs. Following, the power spectrogram of each CRF were correlated with the power spectrogram of bird song stimuli to locate maximum cross-correlation/peak activation of each CRF with the stimuli. Figure 9(a) demonstrates a spatial-temporal map of peak activation of eight cell CRFs corresponding to 60 s of bird song. Ultimately, we were able to reconstruct bird song stimuli portions with this method by finding location of CRFs corresponding to specific portions of vocal elements of stimuli] (figure 9(b)). These methods are explained in detail elsewhere [27–29].

4. Discussions and conclusions

In this study, we introduced an origami style neural prosthesis probe that can unfold to a combination of a surface ECoG array and depth shank during brain implantation. This probe referred to as ‘Epi-intra’ has a 2D flat surface part made of a thin flexible polyimide polymer substrate which can conform to the cortex curvature, while the depth shank is reinforced with a thicker durimide layer for easy brain penetration. This 3D style brain recording platform has the ability to cover recordings from a volume of tissue: from the surface to deep brain. The origami nature of the probe, therefore, made it a suitable candidate for studying neural signal propagation, neural coding, and stimuli encoding in 3D volume of brain tissue. The microelectrodes are made of lithographically patterned glassy carbon material that has shown high potential for use in neural applications [9–12, 30–32]. In recent studies, we have shown not only the GC microelectrodes are chemically inert, biocompatible, electrochemically stable under prolonged electrical stimulation, and have high signal-to-noise ratio (SNR) [10, 12], but also -they exhibit high sensitivity for electrochemical detection of neurotransmitters such as dopamine [12, 32].

Here, we have demonstrated that the probe is mechanically robust and easy to implant in an animal model (starling bird). The tensile load test showed that the probe can carry more than 10 newtons of tensile load, much higher than any load expected

during surgery. We have also shown through finite element modeling that with a total load of only 10 millinewton, the polyimide flap component of the Epi-Intra probe that contains the surface microelectrodes will open up completely. We have also shown that the maximum stress that occurs during the deployment of the probe is only ~90 MPa which is much less than the tensile yield strength of 200 MPa for the polyimide substrate layer. Histology results also demonstrated that there was minimal tissue damage during the deployment of this 3-dimensional neural probe. Further, *in vivo* experiments using the Epi-Intra probe had shown in high quality single cell and multi-unit electrical recordings of from auditory area of starling bird brain. From these recordings, we were able to determine LFP signals as well as high quality stimulus-locked auditory single cells from both deep brain and cortical surface. It is particularly noteworthy that the surface microelectrodes were able to record single-unit activity (SUA). This particular ability of GC microelectrodes has a major significance, since it directly suggests that the use of only less-invasive surface microelectrodes in micro-electrocorticogram arrays allows single cell recordings that further could be used to reconstruct movement-related intracortical activity from signals recorded at the motor cortex [33].

Taken together, the combination of mechanical robustness and high quality recording in a 3D fashion enabled by this probe, therefore, allowed us to investigate neuronal signal propagation mechanisms between neuronal cells and their relationship with the stimuli and, in the process, elucidate brain responses in a 3D fashion. To investigate the signal propagation mechanism and their relationship with the stimuli, first the correlation between the LFP signals were monitored. The results demonstrate that, although there were high correlation between the surface Epi channels as well as between Intra depth channels themselves, the overall correlation was relatively low among surface and depth channels due to the large distance between cells on the surface and at depth. Therefore, to address this limitations of determining cross-correlations in cells separated by large distances and to subsequently validate the use of the Epi-Intra probe as a tool for neural coding, we proposed the investigation of composite receptive fields of neuron cells.

In a recent study, we have demonstrated that CRFs of neurons are independent of the neurons’ distance, location and, topology [28]. The stimulus-locked properties of recorded cells by the Epi-Intra probe proved to be useful in making them viable candidates for CRFs extraction. There are several prevailing models which can create receptive fields from neuron cells such as spike trigger average (which has been used widely to build linear receptive fields [34], spike-triggered covariance [35], and maximally informative dimensions (MID) [36]. Although

these models provide extensive information about receptive fields, they exhibit limitations such as inability to characterize nonlinear information of stimuli [37], limitation working with natural stimuli such as human speech or bird song [38, 39], and limitations in identifying large numbers of relevant receptive field features with respect to natural stimuli [27].

In contrast, the MNE model utilized in this study overcomes most of these drawbacks [27, 29, 36, 40]. Maximum noise entropy (MNE) model generates CRFs from stimulus-locked neural responses by searching for the highest mutual information between stimuli and the brain response in the form of CRFs [27, 29]. By utilizing the MNE model, therefore, we extracted CRFs from the cells and subsequently categorized them into facilitatory and suppressive responses. Finally, these facilitatory and suppressive CRFs were spatially mapped to their recording sites on the Epi-Intra probe and temporally correlated to the stimuli. From this spatial-temporal map, one can observe neural coding mechanism by spatially following propagation of facilitatory and suppressive CRFs of many cells from deep brain to the surface of the cortex, independent of neuron locations in a 3D volume of brain tissue and also temporally encode and reconstruct stimuli.

Consequently, we submit that the Epi-Intra neural probe offers a compelling platform for study of neural coding and stimuli encoding/reconstruction in a 3D volume of brain tissue. In addition to this unique advantage of providing a platform for elucidating new neuroscience understandings, this probe can have a significant potential for chronic implants and recordings as part of a therapeutic BCI prosthetics, as demonstrated by this and our prior reported studies.

Acknowledgments

This material is based on research work supported by the Center for Neurotechnology (CNT), a National Science Foundation Engineering Research Center (EEC-1028725), and ONR (Dynamics of Multifunction Brain Network).

Author contributions

N.W.V. designed the experiments, assisted the recordings, performed the analysis, contributed to design of probes, and wrote the manuscript. S.R. performed the recordings. E.C., C.C. and S.N. designed the probes. C.C. microfabricated and *in vitro* characterized the probes. R.Y. and R.A. performed the mechanical load test. S.K., T.Q.G., and S.A.D contributed to the experimental design and edited the manuscript. S.K. wrote the Methods section.

ORCID iDs

Nasim W Vahidi  <https://orcid.org/0000-0002-9065-2488>

Elisa Castagnola  <https://orcid.org/0000-0001-8070-4777>

Sam Kassegne  <https://orcid.org/0000-0002-6418-000X>

References

- [1] Juavinett A L and Bekheet G 2019 Chronically implanted Neuropixels probes enable high-yield recordings in freely moving mice *Elife* **8** e47188
- [2] Dutta B et al 2019 The Neuropixels probe: a CMOS based integrated microsystems platform for neuroscience and brain-computer interfaces 2019 *IEEE Int. Electron Devices Meeting* pp 10.1.1–4
- [3] Chiang C et al 2020 Development of a neural interface for high-definition, long-term recording in rodents and nonhuman primates *Sci. Transl. Med.* **12** eaay4682
- [4] Khodagholy D, Gelinas J N, Thesen T, Doyle W, Devinsky O, Malliaras G G and Buzsáki G 2015 NeuroGrid: recording action potentials from the surface of the brain *Nat. Neurosci.* **18** 310–5
- [5] Paulk A C et al 2020 Microscale physiological events on the human cortical surface detected with PEDOT:PSS electrodes *bioRxiv* 770743 (submitted) (<https://doi.org/10.1101/770743>)
- [6] Liu R et al 2017 High density individually addressable nanowire arrays record intracellular activity from primary rodent and human stem, cell derived neurons *Nano Lett.* **17** 2757–64
- [7] Hermiz J et al 2020 Stimulus driven single unit activity from micro-electrocorticography *Frontiers Neurosci.* **14** 55
- [8] Khodagholy D, Doublet T, Gurfinkel M, Quilichini P, Ismailova E and Leleux P 2011 Highly conformable conducting polymer electrodes for *in vivo* recordings *Adv. Mater.* **23** H268–H272
- [9] Vomero M, Van Niekerk P, Nguyen V, Gong N, Hirabayashi M, Cinopri A and Kassegne S 2016 A novel pattern transfer technique for mounting glassy carbon microelectrodes on polymeric flexible substrates *J. Micromech. Microeng.* **26** 025018
- [10] Vomero M, Castagnola E, Ciarpella F, Maggiolini E, Goshi N, Zucchini E and Ricci D 2017 Highly stable glassy carbon interfaces for long-term neural stimulation and low-noise recording of brain activity *Sci. Rep.* **7** 40332
- [11] Goshi N, Castagnola E, Vomero M, Gueli C, Cea C, Zucchini E and Fadiga L 2018 Glassy carbon MEMS for novel origami-styled 3D integrated intracortical and epicortical neural probes *J. Micromech. Microeng.* **28** 065009
- [12] Nimbalkar S, Castagnola E, Balasubramani A, Scarpellini A, Samejima S, Khorasani A and Kassegne S 2018 Ultra-capacitive carbon neural probe allows simultaneous long-term electrical stimulations and high-resolution neurotransmitter detection *Sci. Rep.* **8** 6958
- [13] Johnson K O 2000 Neural coding *Neuron* **26** 563–6
- [14] Krahe R, Kreiman G, Gabbiani F, Koch C and Metzner W 2002 Stimulus encoding and feature extraction by multiple sensory neurons *J. Neurosci.* **22** 2374–82
- [15] Mesgarani N S 2009 Influence of context and behavior on stimulus reconstruction from neural activity in primary auditory cortex *J. Neurophysiol.* **102** 3329–39
- [16] Hirabayashi M, Logan K, Deutschman C P, McDowell T W, Torres M, Pullman D and Kassegne S 2018 Investigation of interface bonding mechanisms between glassy carbon microelectrodes and polyimide substrate through Fourier

- transform infrared spectroscopy *J. Electrochem. Soc.* **165** B3060-B3070
- [17] Masamoto K and Kanno I 2012 Anesthesia and the quantitative evaluation of neurovascular coupling *J. Cereb. Blood Flow Metab.* **32** 1233–47
- [18] Ayala Y A and Malmierca M S 2012 Stimulus-specific adaptation and deviance detection in the inferior colliculus *Frontiers Neural Circuits* **6** 89
- [19] Chung J E, Magland J F, Barnett A H, Tolosa V M, Tooker A C, Lee K Y and Greengard L F 2017 A fully automated approach to spike sorting *Neuron* **95** 1381–94.e6
- [20] HD Microsystems 2009 HD-4100 Series Product Bulletin Parlin, New Jersey (http://web.mit.edu/scholvin/www/nt245/Documents/resists.HD-4100_ProcessGuide.pdf)
- [21] Technical Product Information Durimide® 7500 Photosensitive Polyimide Precursor, FujiFilm, Japan www.fujifilmusa.com/shared/bin/Durimide%207500_US12.pdf
- [22] Ganji M, Elthakeb A T, Tanaka A, Gilja V, Halgren E and Dayeh S A 2017 Scaling effects on the electrochemical performance of poly (3, 4-ethylenedioxythiophene (PEDOT), Au, and Pt for electrocorticography recording *Adv. Funct. Mater.* **27** 1703018
- [23] Dayan P and Abbott L 2000 *Theoretical Neuroscience* (Cambridge, MA: Massachusetts Institute of Technology)
- [24] Blackwell J M, Taillefumier T O, Natan R G, Carruthers I M, Magnasco M O and Geffen M N 2016 Stable encoding of sounds over a broad range of statistical parameters in the auditory cortex *Eur. J. Neurosci.* **43** 751–64
- [25] Destexhe A, Contreras D and Steriade M 1999 Spatiotemporal analysis of local field potentials and unit discharges in cat cerebral cortex during natural wake and sleep states *J. Neurosci.: Off. J. Soc. Neurosci.* **19** 4595–608
- [26] Bédard C, Kröger H and Destexhe A 2004 Modeling extracellular field potentials and the frequency-filtering properties of extracellular space *Biophys. J.* **86** 1829–42
- [27] Kozlov A S and Gentner T Q 2016 Central auditory neurons have composite receptive fields *Proc. Natl Acad. Sci.* **113** 1441–6
- [28] Vahidi N W 2019 Tools to investigate composite receptive fields in songbird auditory region *Doctoral Dissertation* University of California San Diego
- [29] Fitzgerald J D, Rowekamp R J, Sincich L C and Sharpee T O 2011 Second order dimensionality reduction using minimum and maximum mutual information models *PLoS Comput. Biol.* **7** e1002249
- [30] Hirabayashi M, Mehta B, Nguyen B and Kassegne S 2015 DNA immobilization on high aspect ratio glassy carbon (GC-MEMS) microelectrodes for bionanoelectronics applications *Microsyst. Technol.* **21** 2359–65
- [31] Vahidi N W, Hirabayashi M, Mehta B, Rayatparvar M, Wibowo D, Ramesh V and Kassegne S 2014 Bionanoelectronics platform with DNA molecular wires attached to high aspect-ratio 3D metal microelectrodes *ECS J. Solid State Sci. Technol.* **3** Q29–Q36
- [32] Castagnola E et al 2018 *In vivo* dopamine detection and single unit recordings using intracortical glassy carbon microelectrode array *MRS Adv.* **3** 1629–34
- [33] Khodagholy D et al 2015 NeuroGrid: recording action potentials from the surface of the brain *Nat. Neurosci.* **18** 310–315
- [34] De Boer R and Kuyper P 1968 Triggered correlation *IEEE Trans. Biomed. Eng.* **15** 169–79
- [35] Schwartz O, Chichilnisky E J and Simoncelli E P 2018 Characterizing neural gain control using spike-triggered covariance *Adv. Neural Inf. Process. Syst.* **14** 269–76
- [36] Sharpee T, Rust N C and Bialek W 2004 Analyzing neural responses to natural signals: maximally informative dimensions *Neural Comput.* **16** 223–50
- [37] Theunissen F E, Sen K and Doupe A J 2000 Spectral-temporal receptive fields of nonlinear auditory neurons obtained using natural sounds *J. Neurosci.: Off. J. Soc. Neurosci.* **20** 2315–31
- [38] Schwartz O, Pillow J W, Rust N C and Simoncelli E P 2006 Spike-triggered neural characterization *J. Vis.* **6** 13
- [39] Eggermont J J, Epping W J M and Aertsen A M H J 1983 Stimulus dependent neural correlations in the auditory midbrain of the grassfrog (*Rana temporaria* L.) *Biol. Cybern.* **47** 103–17
- [40] Bialek W, De Ruyter Van Steveninck R R and Tishby N 2006 Efficient representation as a design principle for neural coding and computation 2006 *IEEE Int. Symp. Information Theory* pp 659–63